

Property Modelling

Proposal of the Boltzmann-like superposition principle for nonlinear tensile creep of thermoplastics

Jan Kolařík^{a,*}, Alessandro Pegoretti^b

^a*Institute of Macromolecular Chemistry ASCR, v. v. i., 162 06 Prague 6, Czech Republic*

^b*Department of Materials Engineering and Industrial Technologies, University of Trento, 38100 Trento, Italy*

Received 24 January 2008; accepted 12 March 2008

Abstract

The Boltzmann superposition principle (BSP) valid for “standard linear solids” is presented in all textbooks on viscoelasticity. In practice, the BSP is not applicable to viscoelastic polymers because (i) the apparent limit (if any) of the stress–strain linearity is very low, (ii) real deformations (stresses) are not infinitesimal, and (iii) tensile deformations give rise to additional free volume, which affects all currently running deformation processes. Consistent application of the free volume approach, including the strain-induced free volume, allowed us to derive and verify a new type of the internal time–tensile strain superposition for a series of single-step nonlinear creeps [J. Kolařík, A. Pegoretti, Nonlinear tensile creep of polypropylene: time–strain superposition and creep prediction, *Polymer* 47 (1) (2006) 346]. The Boltzmann-like superposition principle for multistep nonlinear tensile creep, proposed in this paper, consists of (i) the separation of individual creeps, (ii) their reconstruction for the initial free volume by introducing a specific internal time, and (iii) the superposition of the reconstructed creeps. The procedure is demonstrated using creep data for three types of commercial polypropylene.

© 2008 Elsevier Ltd. All rights reserved.

Keywords: Multistep nonlinear tensile creep; Free volume; Internal time–tensile strain superposition

1. Introduction

Creep measurements and predictions are of great practical importance in any application where polymeric materials must sustain loads for long periods of time and maintain their dimensional stability. Theoretical background of the creep behavior of polymers has been well elaborated in the framework of linear viscoelasticity [1–10], which

presumes a linear relation between acting stress and produced strain. The existing models are mainly phenomenological and have no direct relation to molecular composition and structure. Ideally, materials are assumed to be homogeneous and rheologically simple, and imposed deformations infinitesimally small. To this end, an idealized term of “standard linear solid” (SLS) was introduced [4,7,8], which meets all requirements of the theory of linear viscoelasticity. Linearity implies that material constants (functions) are stress and strain independent, so that there is no interaction between responses to preceding and succeeding loadings (excitations).

*Corresponding author. Tel.: +420 296 809 330;
fax: +420 296 809 410.

E-mail address: kolarik@imc.cas.cz (J. Kolařík).

However, it is generally known that the apparent limit of the linear stress–strain relationship of most (in particular crystalline) thermoplastics does not exceed a few tenths of percentage. Beyond this limit, the produced strain typically rises more than linearly with the acting stress [4,5,11–16]. The concept of the linearity limit tacitly implies that there is a “break” (discontinuity) in some material parameters controlling mechanical behavior, which accounts for markedly differing viscoelastic properties below and above this limit. In our opinion [1], such a limit can be rather arbitrary because its value is likely to depend on the accuracy of the method used: the higher the method accuracy the smaller the strain at which the deviation from the stress–strain linearity is detected. Studying nonlinear creep of a series of six polypropylenes [1] we have shown that if temperature, pressure and uniaxial tensile stress are kept constant, the resulting stress–strain relationship should be nonlinear (compliance rising with strain). A linear relationship (compliance independent of stress or strain) would require that some of the material parameters spontaneously vary with strain (or stress) in an exactly predefined way to transform nonlinearity into linearity. As such a “compensation law” would be very fortuitous, the nonlinear viscoelastic behavior should be viewed as general while the linear one is a rather special case.

The above conclusion is in conformity with numerous experimental findings clearly showing that nonlinear viscoelastic behavior dominates over a major portion of the entire response interval of polymeric materials and plays a key role in most applications. Previously, the stress–strain nonlinearity was tentatively encompassed by introducing an empirical function of stress specific for individual test specimens. An alternative approach consisted in application of empirical power laws and similar analytical relationships [4,7,11,17]. Usually, a functional representation is used in which effects of time and strain (or stress) are considered as separable [4,5]. The multiple integral representation of nonlinear creep operates with mixed terms formally ascribed to the joint contributions of imposed stresses to the final deformation [4,7,11], which seems to lack a clear physical substantiation. Schapery [18], formulating the nonlinear creep by means of the principles of irreversible thermodynamics, introduced a stress-induced shift along the time scale. A generalized form of the time–deformation–temperature superposition [19] employing the concept of the Gibbs energy density

increasing with reversible deformations seems to be rather complicated for practical applications. Some recent approaches to nonlinear viscoelastic creep of polymers use the concept of a “material clock” to describe, how the time dependence is controlled by the current state of the material in the course of a solicitation. The shift factor is introduced to convert the experimental time into the internal time defined for a selected reference state of the material. The quantities presumed to control the material clock are, e.g., free volume [1,12–16,20–23], strain [23], stress [24,25] or configurational internal energy [26,27].

In our opinion, the most useful of these concepts is that of the free-volume-driven internal clock with regard to the fact that the phenomenological theory of viscoelasticity [2–9] has shown that retardation (or relaxation) times can be viewed as controlled by the free volume available for molecular (segmental) motions in polymeric materials. Applying the free-volume approach to the nonlinear tensile creep of PP [1,12], PP/poly(styrene-*co*-acrylonitrile) blends [13] and PP/cycloolefin copolymer blends [14], we have derived a formula for the shift factor, which allows construction of a generalized creep curve over a longtime interval by using the internal time–tensile strain superposition. Thus, we were able [1] (i) to quantitatively describe the nonlinear creep behavior by introducing a simple set of material parameters, (ii) to compare the creep behavior of various PPs by employing their generalized compliance curves constructed for a pseudo iso-free-volume state and (iii) to employ the generalized creep curves for prediction of the real time-dependent compliance for selected stresses (lower than the yield stress). The objective of this paper is (i) to employ the previous findings for the analysis of multistep nonlinear tensile creep of PP and (ii) to develop a new Boltzmann-like superposition principle applicable to polymeric materials showing nonlinear viscoelastic behavior.

2. Theoretical background of the proposed approach

The strain in isothermal tensile creep, $\varepsilon(t, \sigma)$, is generally viewed as consisting of three components depending on time t and stress σ [1,4–12]: (i) elastic (instantaneous, reversible) $\varepsilon_e(\sigma)$; (ii) viscoelastic (time-dependent, reversible) $\varepsilon_v(t, \sigma)$; (iii) plastic (irreversible) $\varepsilon_p(t, \sigma)$:

$$\varepsilon(t, \sigma) = \varepsilon_e(\sigma) + \varepsilon_v(t, \sigma) + \varepsilon_p(t, \sigma) \quad (1)$$

If no plastic deformation is produced in the course of creeping, the tensile compliance $D(t, \sigma) = \varepsilon(t, \sigma)/\sigma$, for the isothermal creep generally reads

$$D(t, \sigma) = D_e(\sigma) + D_v(t, \sigma) \quad (2)$$

Linear stress–strain behavior implies that magnitudes of the creep components are exactly proportional to the magnitude of the applied stress, so that a creep compliance $D(t) = \varepsilon(t)/\sigma$ can be defined as a function of time only [4,5]. Isothermal creep (without any irreversible component) of apparently linear viscoelastic materials was reported [4,5,11] to obey, e.g., the Nutting empirical equation

$$\varepsilon(t, \sigma) = K_N \sigma t^p \quad (3)$$

$$D(t) = \varepsilon(t, \sigma)/\sigma = K_N t^p \quad (4)$$

where K_N is a constant and $0 < p \leq 1$ is the creep curve shape parameter reflecting the distribution of retardation times. The spectrum of retardation times corresponding to t^p can be found in Ref. [11].

2.1. The Boltzmann superposition principle for standard linear solids

This principle (BSP) applied to the linear creep states [4–8] that the response of a material to a given load is independent of responses of the material to any load already acting on the material. Thus, each loading step makes an independent contribution to the final strain, so that the total strain is obtained by the addition of all the contributions. In other words, the BSP states that the effect of a compound cause is the sum of effects of the individual causes [8]. Another consequence of the BSP [4] is that creep recovery is a reversal (“mirror image”) of the preceding creep [7], i.e., creep and recovery are identical in magnitude. All these requirements are met by the (hypothetical) standard linear solid at infinitesimal strains [4,7]. In the case of time-dependent materials, the strain $\varepsilon(t, \sigma)$ is linearly proportional to the applied stress σ , when produced strains are compared at equivalent periods of time t , elapsed after respective loadings. Thus, compliance curves $D(t) = \varepsilon(t, \sigma)/\sigma$ as a function of time detected for various stresses are identical, i.e. independent of applied stress. It is worth noting that the form of the dependence on time is irrelevant. The formulation of the BSP for a multistep creep of linear viscoelastic solids under isothermal conditions

reads [4,5]

$$\varepsilon(t_i, \sigma) = D(t_j)\sigma_1 + D(t_j - t_1)\Delta\sigma_2 + \dots + D(t_j - t_{k-1})\Delta\sigma_k \quad (5)$$

where stress σ_1 is acting since $t_j = 0$, added stress $\Delta\sigma_2$ since $t_j = t_1$, etc. The stresses of concern are the incremental stresses $\Delta\sigma_i$ ($1 < i \leq k$). The validity of the BSP means that the additional creep produced by stress $\Delta\sigma_i$, added in time t_j is identical with the creep which would occur if no other loadings were applied before time t_j .

2.2. Nonlinear tensile creep as a function of the fractional free volume

So far, the effects of temperature and hydrostatic pressure on linear viscoelastic behavior of polymers have quantitatively been interpreted [3–10] in terms of the fractional free volume f available for molecular (segmental) mobility. We have shown [12–16] that a plausible concept of nonlinear viscoelasticity can also be based on the consistent application of the free volume approach. It is generally known that an isotropic solid body with Poisson’s ratio $\nu < 0.5$ dilates when deformed in tension [5–9]. As the strain-induced increment in the specific volume can be identified with the increment in the free volume [28–30], the molecular mobility in polymers becomes dependent on the tensile strain. The contributions to the fractional free volume f produced by increasing temperature (above the glass transition temperature T_g), Δf_T , and tensile strain Δf_ε are expressed by the following equations (1, 3, 5)

$$\begin{aligned} f(T, t_j) &= f_g + \Delta f_T(T) + \Delta f_\varepsilon(t_j) \\ &= f_g + \alpha_{fv}(T - T_g) + (1 - 2\nu)\varepsilon(t_j) \end{aligned} \quad (6)$$

where f_g is the fractional free volume in the glassy state (customarily viewed [3–10] as an iso-free-volume state with f_g around 0.025) and α_{fv} is the expansion coefficient of the free volume, which can be approximated as the difference between the expansion coefficients above and below T_g , i.e., $\alpha_{fv} = \alpha_1 - \alpha_g$. At a constant temperature, pressure and stress, $f(t_j)$ is proportional to the achieved strain $\varepsilon(t_j)$:

$$f(t_j) = Q + k\varepsilon(t_j) \quad (7)$$

where $Q = (f_g + \Delta f_{Tc})$, $k = M(1 - 2\nu)$ and M is the strain magnification factor of the most creeping phase in samples consisting of 2 or 3 phases. M is

evaluated as the mean ratio of the strain calculated for the creeping (e.g. amorphous) phase and of the measured strain. Details on the calculations using the equivalent box model are given in Refs. [12,14].

The available f controls [2–5] retardation (or relaxation) times τ of polymers:

$$\ln \tau(f) = \ln \Omega + (B/f) \tag{8}$$

where Ω corresponds to the frequency of thermal motion inside a potential well and $B \cong 1$ is a numerical factor related to the ratio of the volume of a jumping segment and of the volume of critical vacancy necessary for a segment jump. The effect of changes in f on a retardation time $\tau(f)$ is routinely expressed by means of a shift factor along the logarithmic time scale [2–9]. The time–strain shift factor $\log a_\varepsilon(\tau)$ defined as the ratio of the retardation time $\tau(f_j)/\tau(f_0)$ at different strains can be formulated [1,12] in terms of the mean retardation time τ_m (at a constant temperature T_c) considering two states: (i) $\tau_m[\varepsilon(t_j), T_c]$ for a strain $\varepsilon(t_j)$ achieved at time t_j ; (ii) τ_{m0} for a reference strain $\varepsilon(t_0)$ at time t_0 . With regard to Eq. (8), the shift factor between the two states is

$$\begin{aligned} \log a_\varepsilon(\tau) &= \log \tau_m(f_j) - \log \tau_{m0}(f_0) \\ &= -B'[f(t_j) - f(t_0)]/[f(t_j)f(t_0)] \end{aligned} \tag{9a}$$

where $B' = (B/2.303)$. In full notation

$$\log a_\varepsilon(\tau) = -B'k[\varepsilon(t_j) - \varepsilon(t_0)]/[Q + k\varepsilon(t_j)][Q + k\varepsilon(t_0)] \tag{9b}$$

The following semiempirical equation relating compliance to time and stress was found appropriate for a number of thermoplastics [1,12–16,31]

$$D(t, \sigma) = W(\sigma)(t/\tau_m)^n \tag{10}$$

where $W(\sigma)$ is a function of acting stress and n has an analogous meaning to p in Eqs. (3) and (4). Combining Eqs. (9a, 9b) and (10) and separating the effects of time and stress we obtain [1,12]

$$\begin{aligned} \log D(u_j) &= [\log W(\sigma) - n \log \tau_{m0}] + n[\log t_j - \log a_\varepsilon(\tau)] \\ &= \log C + n \log u_j \end{aligned} \tag{11}$$

where $u_j = t_j/a_\varepsilon(\tau)$ denotes the “internal time” in a creep experiment. Combining Eqs. (9a) and (11) we obtain

$$\begin{aligned} \log u_j &= \log t_j + B'k[\varepsilon(t_j) - \varepsilon(t_0)]/[Q + k\varepsilon(t_j)] \\ &\quad \times [Q + k\varepsilon(t_0)] \end{aligned} \tag{12}$$

It is to be noted that $\log D(t_j) = \log D(u_j)$ is valid for corresponding t_j and u_j . The $\log D(t_j)$ vs. $\log t_j$ plot would coincide with the corresponding $\log D(u_j)$ vs. $\log u_j$ plot for extremely low (infinitesimal) stresses and strains ($\Delta f_\varepsilon \rightarrow 0$); thus C and n represent the limiting values for a hypothetical creep in the iso-free-volume state. Obviously, such dependence for infinitesimal strains cannot be obtained experimentally, because of the accuracy and time limits of real creep measurements.

Eq. (11) anticipates a linear dependence $\log D(u_j)$ vs. $\log u_j$, which, however, does not correspond to the linear viscoelasticity. Alternatively, we used a polynomial of the second degree instead of Eq. (11) to fit some types of the $\log D(u)$ vs. $\log u$ dependences

$$\log D(u) = \log C_h + (a + b \log u) \log u \tag{13}$$

So far we have found $b = 0$ for various types of PP [1,12], $b < 0$ for high-density polyethylene HDPE [16] and $b > 0$ for poly(ethylene terephthalate) PET [15]. Our extensive results for these polymers brought evidence that $\log C$ and n (or $\log C_h$, a and b) are independent of stress (or strain), which is in conformity with the concept that $\log C$ and n are the limiting values for creep in the (hypothetical) iso-free-volume state.

3. Experimental section

3.1. Tested polypropylenes

Structure and creep behavior of the tested polypropylenes produced by Basell, Ferrara, Italy were fully characterized in our previous paper [1]. Briefly, Moplen C30G is isotactic polypropylene recommended for the production of injection-molded parts (crystallinity: 44.4%). Moplen RP210G is a random copolymer with 3% of ethylene, designed for blow molding and sheet extrusion. Due to lower crystallinity (36.5%), it shows more profound viscoelastic behavior than ordinary PP. Moplen EPT30R is a “reactor” blend consisting of 88% of isotactic polypropylene (crystallinity: 42.2%) and 12% of ethylene/propylene rubber. This rubber-toughened polypropylene was prepared by a two-step polymerization reaction, so that spherical domains of rubber are evenly distributed in PP matrix and bound by covalent bonds [32]. EPT30R was selected in order to verify the validity of the proposed approach for a three-phase material. Preparation of injection-molded

dumb-bell test specimens (ISO 527) was described in the previous papers [12–16,32].

3.2. Tensile creep measurements

Tensile creep was measured using an apparatus equipped with a mechanical stress amplifier (lever) 10:1. A mechanical strain gauge (accuracy of about $2\mu\text{m}$) was connected to the upper clamp of the specimen to indicate the displacement. Specimen dimensions: initial distance between grips 90 mm; cross-section $10\text{ mm} \times 4\text{ mm}$. Specimens were stored for more than 2 years at room temperature (cf. [1]) so that possible interfering effect of physical aging during creep measurements was excluded. Creep tests were performed at $23 \pm 0.3^\circ\text{C}$, i.e., about 30 K above the T_g of PP. Mechanical conditioning preceding a measurement consisted of applying a stress (for 300 min) equal to or higher than the highest stress applied in the following three-step creep (which was implemented after a 48 h recovery). Three-step creep measurements were performed at three progressively increasing stress levels: σ_1 , $\sigma_1 + \Delta\sigma_2$, $\sigma_1 + \Delta\sigma_2 + \Delta\sigma_3$.

4. Results and discussion

4.1. Multistep nonlinear tensile creep (MSC)

In this paper, we will mainly analyze relatively simple nonlinear three-step creeps executed with stresses σ_1 , $\Delta\sigma_2$, $\Delta\sigma_3$ acting in time intervals $0 < t_j \leq t_3$, $t_1 < t_j \leq t_3$, $t_2 < t_j \leq t_3$, respectively, where $t_1 = 100$, $t_2 = 200$, $t_3 = 300$ min. Alternatively, creep experiments were carried out for unequal time intervals, e.g. $t_1 = 50$, $t_2 = 150$, $t_3 = 1000$ min. The first step necessary for processing experimental data is the separation of strains produced by creeps #1–3. Fig. 1a illustrates the total creep strain and strains of separated individual creeps as function of time. The strain $\varepsilon_1(t_j)$ produced by creep #1 is identical with the total strain $\varepsilon(t_j)$ used for calculating $\log D_1(t_j)$ in the interval $0 < t_j \leq t_1$. As soon as $\varepsilon_1(t_j)$ is extrapolated for $t_1 < t_j \leq t_2$, the strain $\varepsilon_2(t_j - t_1) = \varepsilon(t_j) - \varepsilon_1(t_j)$ and corresponding compliance $\log D_2(t_j - t_1)$ of creep #2 in the second time interval $t_1 < t_j \leq t_2$ can be calculated. Analogously, the extrapolation of $\varepsilon_1(t_j)$ and $\varepsilon_2(t_j - t_1)$ for $t_2 < t_j \leq t_3$ permits the calculation of $\varepsilon_3(t_j - t_2) = \varepsilon(t_j) - \varepsilon_1(t_j) - \varepsilon_2(t_j - t_1)$ and

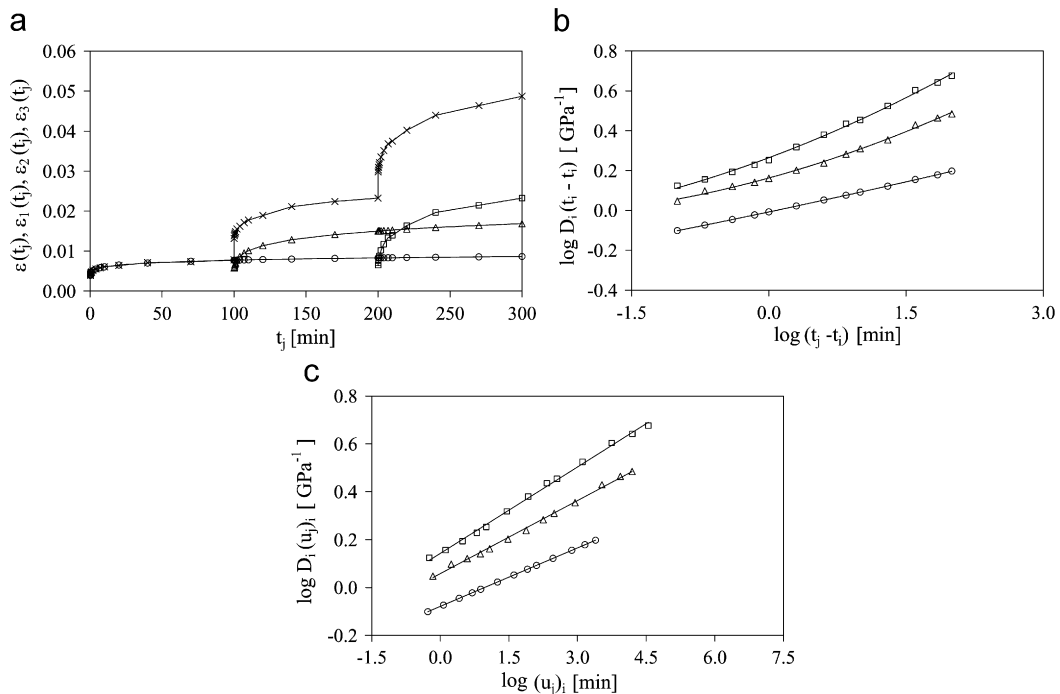


Fig. 1. Three-step tensile creep of Moplen RP210G for $\sigma_1 = \Delta\sigma_2 = \Delta\sigma_3 = 4.90\text{ MPa}$ imposed at 0, 100, and 200 min, respectively. (a) Creep strain plotted against real time: total strain $\varepsilon(t_j)$ (x); strains produced by creeps #1, 2, and 3, respectively: $\varepsilon_1(t_j)$ (○); $\varepsilon_2(t_j - t_1)$ (△); $\varepsilon_3(t_j - t_2)$ (□). (b) Creep compliance plotted against respective real time: $\log D_1(t_j)$ (○); $\log D_2(t_j - t_1)$ (△); $\log D_3(t_j - t_2)$ (□). (c) Creep compliance plotted against respective internal time defined by Eqs. (15a–15c): $\log D_1(u_j)_1$ (○); $\log D_2(u_j)_2$ (△); $\log D_3(u_j)_3$ (□). Input parameters [1]: $B = 1$; $M = 1.40$; $\nu = 0.4$; $Q = 0.025$.

log $D_3(t_j - t_2)$ produced by creep #3 in the third time interval $t_2 < t_j \leq t_3$. The strain extrapolation of creep #1 (or #2) is based on plots of experimental data $\varepsilon_1(t_j)$ [or $\varepsilon_2(t_j - t_1)$] against log t_j [or log $(t_j - t_1)$] in the interval $0 < t_j \leq 100$ (or $100 < t_j \leq 200$); individual plots are fitted with a polynomial of the second degree, which is then used for strain calculation at the following time intervals. It is to be noted that e.g. creep #1 is independently measured over three decades of time (i.e. 0.1–100 min), while the following extrapolation (from 100 to 300 min) extends over about one half of the time decade. Nonetheless, the accuracy of the strain or compliance data may decrease with the creep number, due to accumulating extrapolations and deductions.

Compliances characterizing creeps #1–3 executed with $\sigma_1 = \Delta\sigma_2 = \Delta\sigma_3$ are plotted against real time in Fig. 1b: in the first interval $-1 < \log t \leq 2$ (i.e., 0.1–100 min), a simple creep #1 takes place and log $D_1(t_j)$ is plotted against log t_j . Analogously, log $D_2(t_j - t_1)$ of creep #2 and log $D_3(t_j - t_2)$ of creep #3 are plotted against log $(t_j - t_1)$ and log $(t_j - t_2)$, respectively, over the intervals $t_1 < t_j \leq t_2$ and $t_2 < t_j \leq t_3$. As expected, the compliance of the individual creeps notably increases with the creep number due to the nonlinearity of the viscoelastic behavior of PP. The addition of any load increases the total creep strain and, consequently, the available fractional free volume $f(t_j)$ which controls the dynamics of all concurrently running creeps. For this reason, creeps #1–3 are not independent of each other, but necessarily interact. As explained before, a relevant comparison of nonlinear creeps and their potential superposition necessitate the compliance plots against respective internal times. In contrast to a series of single-step nonlinear tensile creeps (SSC), the starting values of free volumes of individualized creeps in a MSC are not identical, but have to be identified with those at $t = 0$, $t = t_1$, $t = t_2$. Then shift factors due to the strain-induced free volume expansion defined by Eq. (9a) for creeps #1, 2, and 3 in the 1st, 2nd, and 3rd time intervals, respectively, read

$$\log a_{e1}(\tau) = -B'[f(t_j) - f(t_0)]/[f(t_j)f(t_0)] \quad \text{for } t_0 < t_j \leq t_1 \quad (14a)$$

$$\log a_{e2}(\tau) = -B'[f(t_j) - f(t_1)]/[f(t_j)f(t_1)] \quad \text{for } t_1 < t_j \leq t_2 \quad (14b)$$

$$\log a_{e3}(\tau) = -B'[f(t_j) - f(t_2)]/[f(t_j)f(t_2)] \quad \text{for } t_2 < t_j \leq t_3 \quad (14c)$$

Corresponding internal times defined by Eq. (12) are then the following:

$$\log(u_j)_1 = \log t_j + B'\{k[\varepsilon(t_j) - \varepsilon(t_0)]\} / \{[Q + k\varepsilon(t_j)][Q + k\varepsilon(t_0)]\} \quad (15a)$$

$$\log(u_j)_2 = \log(t_j - t_1) + B'\{k[\varepsilon(t_j) - \varepsilon(t_1)]\} / \{[Q + k\varepsilon(t_j)][Q + k\varepsilon(t_1)]\} \quad (15b)$$

$$\log(u_j)_3 = \log(t_j - t_2) + B'\{k[\varepsilon(t_j) - \varepsilon(t_2)]\} / \{[Q + k\varepsilon(t_j)][Q + k\varepsilon(t_2)]\} \quad (15c)$$

Fig. 1c shows that the log $D_i(u_j)_i$ vs. log $(u_j)_i$ plots are virtually linear, very much like in a series of SSC [1]. At the same time it can be seen that (i) the initial compliance, (ii) the slope of the dependences and (iii) the internal time interval increase with the creep number. Thus additional steps—in comparison with a series of SSC—should be taken to implement the superposition of individualized creeps.

4.2. Superposition of the creeps obtained via the dissolution of a three-step creep

First, we will briefly review the existing concepts of the creep superposition in order to single out specific features of the approach proposed in this paper. If stresses σ_1 , $\Delta\sigma_2$, and $\Delta\sigma_3$ were acting on the SLS in time intervals $0 < t_j \leq t_3$, $t_1 < t_j \leq t_3$, $t_2 < t_j \leq t_3$, respectively, the produced dependences log D_1 vs. log t_j , log D_2 vs. log $(t_j - t_1)$ and log D_3 vs. log $(t_j - t_2)$ would be identical over the first 100 min of each creep, i.e. individual creeps #1, 2, and 3 from the multistep experiment would coincide. Naturally, as creeps of the SLS are independent of each other, the observed dependences would be identical with those produced in the single-step creep.

Polymer solids showing nonlinear viscoelastic properties are very different from the SLS: (i) their response to a load depends on loads already acting; (ii) simultaneously running creeps interact with one another (due to the controlling role of the actual free volume), which invalidates their additivity; (iii) recovery is not a reversal of the preceding creep because $f(t_j)$ rises with time in the course of the creep, while decreases during the recovery. For these reasons [1,12], the time–strain superposition of single-step nonlinear tensile creeps cannot be achieved by using plots against real time, but internal time has to be introduced. The superposition works well for a series of SSC, i.e. the log $D(u_j)$ vs. log (u_j) dependences obtained for different

stresses superpose in one generalized dependence over an extended scale of internal time [1,12], if the reference state is identified with the initial non-deformed state. We have also shown [1,14,16] that the generalized creep curve obtained through the internal time–tensile strain superposition is in very good accord with experimental long-term creep curves. To implement this superposition, the horizontal shift factors $a_e(\tau)$ are to be calculated *a priori* for each point of the superposed compliance dependences since $a_e(\tau)$ grows with the free volume in a creeping specimen, due to the rising creep strain $\varepsilon(t_j)$. It is worth noting that the vertical shifts used, e.g., in the time–temperature superposition [2–7] do not enter the internal time–strain superposition because the creep temperature is constant and the decrease in specimen density, due to the strain-induced expansion in the course of creep experiments, is virtually negligible.

Analogous superposition of the individual non-linear creeps obtained via the dissolution of a MSC is much more complex because several facts have to be taken into account: (i) actual $f(t_j)$, which controls the scales of the internal times of all simultaneously running creeps, is continuously increasing in proportion to *total* strain $\varepsilon(t_j)$ according to Eq. (7); (ii) imposition of an additional load produces a step-like increase in $\varepsilon(t_j)$ and $f(t_j)$; (iii) individual creeps start at different $f(t_j)$ and proceed at different free volume levels. While the effect of $f(t_j)$ on $\log u_j$ can be described quantitatively by means of Eqs. (15a–15c), $\log D(u_j)$ depending on $f(t_j)$ and the loading history can be anticipated only qualitatively. The latter fact necessitates the usage of the compliance experimental data in the following superposition of separated creeps #1–3.

As expected, in a series of SSC we observed [1,12–16] that the higher the stress and produced strains (over the creep time interval), the higher the corresponding values of the compliance and shift factor (observed at a certain creep time). However, it is essential to note that the parallel increases in $\log(u_j)$ and $\log D(u_j)$ are “proportional”, i.e. the ratio of the increments $\Delta \log(u_j)$ and $\Delta \log D(u_j)$ over a selected time interval is independent of stress. Consequently, all dependences $\log D(u_j)$ vs. $\log u_j$ coincide and values of $\log C$ and parameter n defined by Eq. (11) are independent of stress. In contrast, in the model MSC with stresses $\sigma_1 = \Delta \sigma_2 = \Delta \sigma_3$ we can observe (Fig. 1c) that increments $\Delta \log D_1(u_j)_1 < \Delta \log D_2(u_j)_2 < \Delta \log D_3(u_j)_3$ (e.g. over the time interval 0.1–100 min of each

creep) are rising faster than the corresponding increments $\Delta \log(u_j)_1 < \Delta \log(u_j)_2 < \Delta \log(u_j)_3$. The reason is that creeps #2 and 3 do not start from the non-deformed state, but their initial compliance is higher in proportion to already existing deformation, which accounts for an “excessive” increase in compliance in the course of these creeps. Nonetheless, it is essential to point out that the observed dependences are linear very much like those in the series of SSC. To apply the previously developed superposition principle [1,12] to individualized creeps from MSC, it is necessary to equalize the slope of the dependences visualized in Fig. 1c. In other words, $\Delta \log(u_j)_i$ should correspond to the observed $\Delta \log D_i(u_j)_i$ in a similar way as in a series of SSC. Considering creep #1 as the “reference” creep in a MSC, the ratio $\Delta \log D_2(u_j)_2 / \Delta \log D_1(u_j)_1$ or $\Delta \log D_3(u_j)_3 / \Delta \log D_1(u_j)_1$ should be taken into account concurrently with the ratio of the corresponding internal time scales. In this respect, any internal time has to be regarded as an entity consisting of two inseparable terms, namely real time and shift factor, which cannot be controlled independently. Using Eqs. (15a–15c) we can formulate the following increments of internal times for creeps #1–3:

$$\begin{aligned} \Delta \log(u_j)_1 &= [\log(t_1) - \log(t_{1s})] + B' [f(t_1) \\ &\quad - f(t_{1s})] / [f(t_1)f(t_{1s})] \\ &= \Delta \log(t_j)_1 + \Delta \log a_{e1}(\tau) \end{aligned} \quad (16a)$$

$$\begin{aligned} \Delta \log(u_j)_2 &= [\log(t_2 - t_1) - \log(t_{2s} - t_1)] \\ &\quad + B' [f(t_2) - f(t_{2s})] / [f(t_2)f(t_{2s})] \\ &= \Delta \log(t_j)_2 + \Delta \log a_{e2}(\tau) \end{aligned} \quad (16b)$$

$$\begin{aligned} \Delta \log(u_j)_3 &= [\log(t_3 - t_2) - \log(t_{3s} - t_2)] \\ &\quad + B' [f(t_3) - f(t_{3s})] / [f(t_3)f(t_{3s})] \\ &= \Delta \log(t_j)_3 + \Delta \log a_{e3}(\tau) \end{aligned} \quad (16c)$$

where t_{1s} , t_{2s} , and t_{3s} are the times for which $\log(u_j)_1 = \log(u_j)_2 = \log(u_j)_3 = 0$, respectively. Subsequently we can estimate the following ratios:

$$\begin{aligned} T_2 &= [\Delta \log(t_j)_1 + \Delta \log a_{e1}(\tau)] / [\Delta \log(t_j)_2 \\ &\quad + \Delta \log a_{e2}(\tau)] \end{aligned} \quad (17a)$$

$$\begin{aligned} T_3 &= [\Delta \log(t_j)_1 + \Delta \log a_{e1}(\tau)] / [\Delta \log(t_j)_3 \\ &\quad + \Delta \log a_{e3}(\tau)] \end{aligned} \quad (17b)$$

The corresponding values of $\Delta \log D_1(u_j)_1$, $\Delta \log D_2(u_j)_2$, and $\Delta \log D_3(u_j)_3$ over the indicated increments of internal times are to be extracted from

experimental data, in order to evaluate the following ratios

$$R_2 = \Delta \log D_1(u_j)_1 / \Delta \log D_2(u_j)_2 \quad (18a)$$

$$R_3 = \Delta \log D_1(u_j)_1 / \Delta \log D_3(u_j)_3 \quad (18b)$$

In analogy to the internal time–tensile strain superposition of a series of SSC [1,12–16], it is obvious that increasing free volume necessarily expands the internal time scales of creeps obtained by the dissolution of a MSC (Fig. 1c). Thus, the “excessive” increase in $\log D(u)$ of creeps #2 and 3 is to be encompassed (“projected” into the internal time scale) through an additional “scale expansion factor” G to maintain the proportionality between the corresponding increments of compliance and internal time. Introducing Eqs. (17a, 17b) and (18a, 18b) into Eqs. (15a–15c) the “transformed internal time” for creep #2 or 3 is obtained:

$$\log(u_j)_1 = \log t_j + B'k[\varepsilon(t_j) - \varepsilon(t_0)] / \{ [Q + k\varepsilon(t_j)] \times [Q + k\varepsilon(t_0)] \} \quad (19a)$$

$$\log(u_j)_{2tr} / G_2 = \log(t_j - t_1) + B'k[\varepsilon(t_j) - \varepsilon(t_1)] / \{ [Q + k\varepsilon(t_j)][Q + k\varepsilon(t_1)] \} \quad (19b)$$

$$\log(u_j)_{2tr} / G_3 = \log(t_j - t_2) + B'k[\varepsilon(t_j) - \varepsilon(t_2)] / \{ [Q + k\varepsilon(t_j)][Q + k\varepsilon(t_2)] \} \quad (19c)$$

where

$$G_2 = T_2 / R_2 \quad (20a)$$

$$G_3 = T_3 / R_3 \quad (20b)$$

Fig. 2a visualizes the compliance plots against the transformed internal times defined by Eqs. (19a–19c). As can be seen, the dependences are parallel, but the discrepancies (gaps) between them are preserved; they can be assigned to different values of $f(t_j)$ at the outset of creeps #1–3. Thus, the shift factor between the starting times of creeps #2 and 1 or creeps #3 and 2 should be added to the shift factors defined in Eq. (19b) or (19c) in order to superpose the transformed compliance curves plotted in Fig. 2a. In this way, the “superposing shift factors” (hence

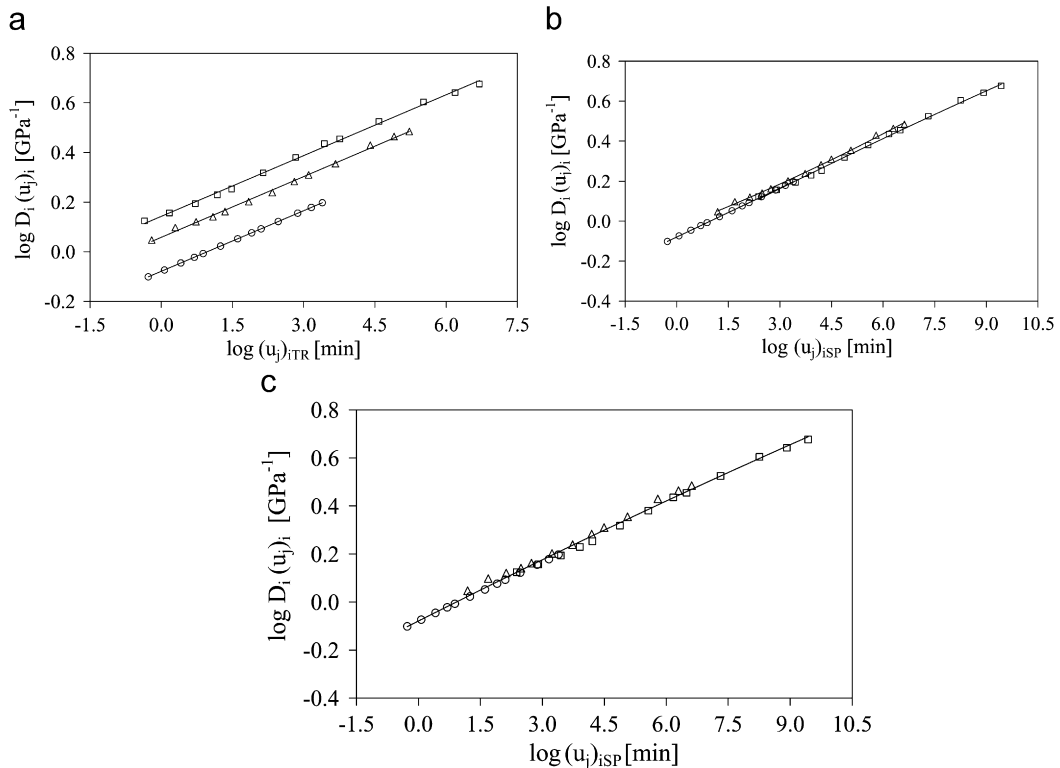


Fig. 2. The internal time–tensile strain superposition of compliances obtained from the three-step tensile creep of Moplen RP210G. $\log D_1(u_j)_1$ (○); $\log D_2(u_j)_2$ (△); $\log D_3(u_j)_3$ (□); applied stresses and input parameters are identical with those given in Fig. 1. (a) Creep compliance plotted against respective transformed internal time defined by Eqs. (19a–19c). (b) Creep compliance plotted against respective superposing internal time defined by Eqs. (21a, 21b). (c) Generalized compliance curve fitting all experimental data of MSC plotted against superposing internal times defined by Eqs. (21a, 21b).

the subscript “sp”) for creep #2 or 3 are obtained. This operation means that the compliance curves #2 and 3 are additionally shifted as an entity in Fig. 2b. It should be noted that the compliance curve of creep #2 is shifted across the interval of the internal time of creep #1 for which $G_1 = 1$. On the other hand, the compliance curve of creep #3 is shifted across the interval of the transformed internal time of creep #2, so that the factor G_2 has to be considered. Thus, the final plots leading to the superposition of creeps #1–3 are the following: $\log D_2(u_j)_2$ is plotted against

$$\log(u_j)_{2sp} = \log(u_j)_{2tr} + B'k[\varepsilon(t_1)/Q]/[Q + k\varepsilon(t_1)] \quad (21a)$$

and $\log D_3(u_j)_3$ against

$$\log(u_j)_{3sp} = \log(u_j)_{3tr} + G_2 B'k[\varepsilon(t_2) - \varepsilon(t_1)] / \{ [Q + k\varepsilon(t_1)][Q + k\varepsilon(t_2)] \} \quad (21b)$$

The final plots in Fig. 2b document that the superposition defined by Eqs. (21a, 21b) is fairly good. Alternatively, the conclusive generalized dependence is visualized in Fig. 2c where all experimental data are considered as an ensemble. The parameters of the generalized dependence, $\log C = -0.06$ and $n = 0.08$, are very close to the values characterizing the generalized dependence obtained through the superposition of a set of SSC in our previous paper [1].

To demonstrate the validity of the proposed superposition principle for MSC, further examples for different sequences of the stress increments and/or different time intervals of individual creeps are given for three types of polypropylenes. Fig. 3 shows a very good superposition obtained for Moplen C306G loaded with $\sigma_1 > \Delta\sigma_2 > \Delta\sigma_3$, where the differences between subsequent stresses are relatively small. A possible effect of much higher stress differences was tested using Moplen EPT30G. Fig. 4 reveals that the superposition is quite satisfactory even when the internal time scales are extended up to much higher values than in the preceding figures. Fig. 5 documents the superposition for $\sigma_1 > \Delta\sigma_2 > \Delta\sigma_3$, where, however, the intervals $t_1 - t_0$, $t_2 - t_1$, and $t_3 - t_2$, are markedly increasing, namely 50, 100, and 1000 min, respectively. Also, in this case, the superposition is quite good despite the fact that relatively short creeps #1 and 2 have to be extrapolated up to the total time corresponding to 1150 min. To test the accuracy of calculations, extremely short intervals of experi-

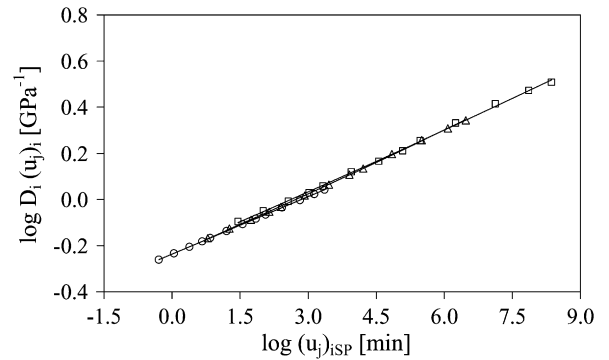


Fig. 3. Three-step tensile creep of Moplen C30G for $\sigma_1 = 6.14$; $\Delta\sigma_2 = 4.91$; $\Delta\sigma_3 = 3.68$ MPa imposed at 0, 100, and 200 min, respectively. Creep compliance plotted against superposing internal time defined by Eqs. (21a, 21b): $\log D_1(u_j)_1$ (\circ); $\log D_2(u_j)_2$ (\triangle); $\log D_3(u_j)_3$ (\square). Input parameters: $B = 1$; $M = 1.54$; $\nu = 0.4$; $Q = 0.025$.

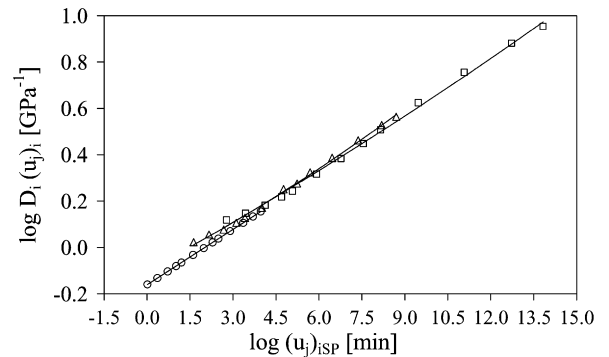


Fig. 4. Three-step tensile creep of Moplen EPT30R for $\sigma_1 = 7.34$; $\Delta\sigma_2 = 4.89$; $\Delta\sigma_3 = 3.67$ MPa imposed at 0, 100, and 200 min, respectively. Creep compliance plotted against superposing internal time defined by Eqs. (21a, 21b): $\log D_1(u_j)_1$ (\circ); $\log D_2(u_j)_2$ (\triangle); $\log D_3(u_j)_3$ (\square). Input parameters: $B = 1$; $M = 1.49$; $\nu = 0.4$; $Q = 0.025$.

mental time were selected, i.e., 20, 50, and 100 min. Fig. 6 shows that even this experiment leads to the plausible superposition, which means that a three-step creep lasting 170 min provides reliable information.

5. Conclusions

The paper is the first to present a successful procedure for the superposition of nonlinear creeps obtained by the dissolution of a multistep creep. The proposed superposition principle is necessarily much more complicated and sophisticated than the Boltzmann superposition principle suggested for

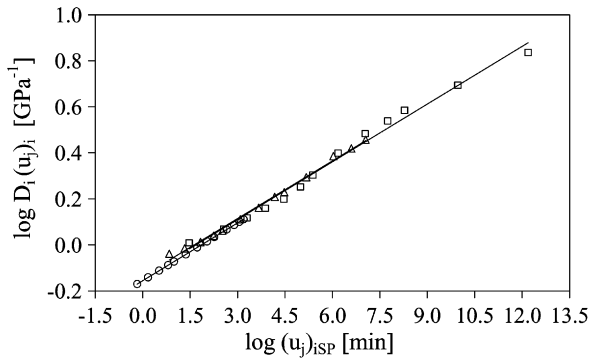


Fig. 5. Three-step tensile creep of Moplen EPT30R for $\sigma_1 = 6.06$; $\Delta\sigma_2 = 3.63$; $\Delta\sigma_3 = 2.42$ MPa imposed at 0, 50, and 150 min and lasting 1150, 1100, and 1000 min, respectively. Creep compliance plotted against superposing internal time defined by Eqs. (21a, 21b): $\log D_1(u_i)_1$ (○); $\log D_2(u_i)_2$ (△); $\log D_3(u_i)_3$ (□). Input parameters: $B = 1$; $M = 1.49$; $\nu = 0.4$; $Q = 0.025$.

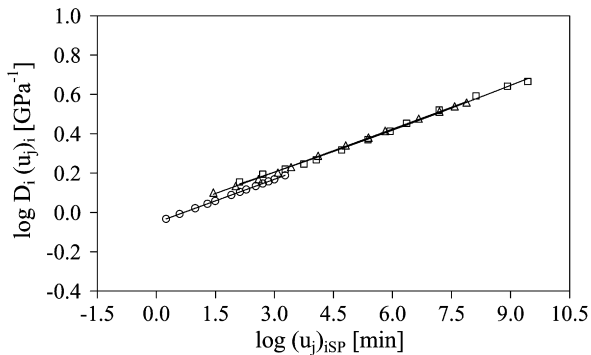


Fig. 6. Three-step tensile creep of Moplen RP210G for $\sigma_1 = 7.38$; $\Delta\sigma_2 = 3.69$; $\Delta\sigma_3 = 2.46$ MPa imposed at 0, 20, and 70 min and lasting 170, 150, and 100 min, respectively. Creep compliance plotted against superposing internal time defined by Eqs. (21a, 21b): $\log D_1(u_i)_1$ (○); $\log D_2(u_i)_2$ (△); $\log D_3(u_i)_3$ (□). Input parameters [1]: $B = 1$; $M = 1.40$; $\nu = 0.4$; $Q = 0.025$.

idealized “standard linear solids”. The free-volume theory of viscoelasticity was used to derive and verify the tensile compliance vs. internal time superposition in the region of nonlinear viscoelastic behavior of polypropylene, poly(propylene-ethylene) and rubber-toughened polypropylene. The used concept assumes that the observed nonlinearity is caused by the strain-induced increment of the free volume. The strain-induced additional free volume rising with the creep strain accounts for shortening of retardation times, which control all concurrently running creeps in MSC.

Our procedure requires the following steps: (i) the dissolution (decomposition) of the total MSC strain into the strains produced by individual creeps; (ii) a

priori point-by-point calculation of internal times for the individualized creeps, which are necessary for comparative plots and their superposition; (iii) as the free volume at the outset of subsequent creeps in MSC increases simultaneously affecting both retardation times and detected compliance, creep #1 is taken as a “reference state” and the subsequent creeps are to be transformed (reconstructed) for the same conditions. After completing these operations, the $\log D_i(u)$ vs. $\log u_i$ dependences of individualized creeps superpose forming a generalized curve (over extended time scale) corresponding to a pseudo iso-free-volume state. The generalized curves obtained from MSC are identical with analogous curves produced via the superposition of a series of SSC [1]. From this point of view, a three-step creep can substitute for a series (say 4–5) of SSC and lead to notable time savings. The generalized $\log D(u)$ vs. $\log u$ dependences can reversely be used for calculating a long-term $\log D(t)$ vs. $\log t$ dependences for any selected stress (in the interval up to the yield stress) as explained in Ref. [1]. The proposed superposition procedure was found viable for all the studied types of PP as well as for various loading sequences and time intervals.

Acknowledgment

The first author (J.K.) is greatly indebted to the Grant Agency of the Academy of Sciences of the Czech Republic for financial support of this work (Institute Grant no. AVOZ 40500505).

References

- [1] J. Kolařík, A. Pegoretti, Nonlinear tensile creep of polypropylene: time-strain superposition and creep prediction, *Polym.* 47 (1) (2006) 346.
- [2] F. Bueche, *Physical Properties of Polymers*, Interscience, New York, 1962.
- [3] J.D. Ferry, *Viscoelastic Properties of Polymers*, Wiley, New York, 1980.
- [4] I.M. Ward, D.W. Hadley, *An Introduction to the Mechanical Properties of Solid Polymers*, Wiley, Chichester, 1993.
- [5] L.E. Nielsen, R.F. Landel, *Mechanical Properties of Polymers and Composites*, M Dekker, New York, 1994.
- [6] F. Rodriguez, *Principles of Polymer Systems*, Taylor & Francis, Washington, DC, 1996.
- [7] R.J. Crawford, *Plastics Engineering*, Butterworth-Heinemann, Oxford, 1998.
- [8] R.S. Lakes, *Viscoelastic Solids*, CRC Press, Boca Raton, FL, 1999.

- [9] E. Riande, R. Diaz-Calleja, M.G. Prolongo, R.M. Masegosa, C. Salom, *Polymer Viscoelasticity*, M. Dekker, New York, 2000.
- [10] D.R. Moore, S. Turner, *Mechanical Evaluation Strategies for Plastics*, Woodhead Publ., Cambridge, 2001.
- [11] W.N. Findley, J.S. Lai, K. Onaran, *Creep and Relaxation of Nonlinear Viscoelastic Materials*, North-Holland Publ. Co., Amsterdam, 1976.
- [12] J. Kolařík, Tensile creep of thermoplastics: time-strain superposition of non-iso-free-volume data, *J. Polym. Sci. B: Polym. Phys.* 41 (7) (2003) 736–748.
- [13] J. Kolařík, A. Pegoretti, L. Fambri, A. Penati, Prediction of nonlinear long-term tensile creep of heterogeneous blends: rubber-toughened polypropylene-poly(styrene-co-acrylonitrile), *J. Appl. Polym. Sci.* 88 (3) (2003) 641–651.
- [14] J. Kolařík, A. Pegoretti, L. Fambri, A. Penati, Nonlinear long-term tensile creep of poly(propylene)/cycloolefin copolymer blends with fibrous structure, *Macromol. Mater. Eng.* 288 (8) (2003) 629–641.
- [15] A. Pegoretti, J. Kolařík, G. Gottardi, A. Penati, Heterogeneous blends of recycled poly(ethylene terephthalate) with impact modifiers: phase structure and tensile creep, *Polym. Int.* 53 (7) (2004) 984–994.
- [16] J. Kolařík, A. Pegoretti, L. Fambri, A. Penati, High-density polyethylene/cycloolefin copolymer blends, part 2: nonlinear tensile creep, *Polym. Eng. Sci.* 46 (10) (2006) 1363–1373.
- [17] M. Schlimmer, Formulierung des mechanischen Werkstoffverhaltens bei zeitabhängiger Spannung-Verformungs-Beziehung, *Rheol. Acta.* 18 (1) (1979) 62–74.
- [18] R.A. Schapery, On the characterization of nonlinear viscoelastic materials, *Polym. Eng. Sci.* 9 (4) (1969) 295–310.
- [19] K.S. Cho, S.Y. Kim, A thermodynamic theory on the nonlinear viscoelasticity of glassy polymers, 1. Constitutive equation, *Macromol. Theory Simulations* 9 (6) (2000) 328–335.
- [20] W.G. Knauss, I. Emri, Volume change and the nonlinearly thermo-viscoelastic constitution of polymers, *Polym. Eng. Sci.* 27 (1) (1987) 86–100.
- [21] G.U. Losi, W.G. Knauss, Free volume theory and nonlinear thermoviscoelasticity, *Polym. Eng. Sci.* 32 (8) (1992) 542–557.
- [22] G.B. McKenna, Y. Leterrier, C.R. Schultheisz, The evolution of material properties during physical aging, *Polym. Eng. Sci.* 35 (5) (1995) 403–410.
- [23] C.F. Popelar, K.M. Liechti, A distortion-modified free volume theory for nonlinear viscoelastic behavior, *Mech. Time-Depend. Mat.* 7 (2) (2003) 89–141.
- [24] J. Lai, A. Bakker, Analysis of the nonlinear creep of high-density polyethylene, *Polym.* 36 (1) (1995) 93–99.
- [25] S. Jazouli, W. Luo, F. Bremand, T. Vu-Khanh, Application of time-stress equivalence to nonlinear creep of polycarbonate, *Polym. Test.* 24 (4) (2005) 463–467.
- [26] J.M. Caruthers, D.B. Adolf, R.S. Chambers, P. Shrikhande, A thermodynamically consistent, nonlinear viscoelastic approach for modeling glassy polymers, *Polym.* 45 (13) (2004) 4577–4597.
- [27] D.B. Adolf, R.S. Chambers, J.M. Caruthers, Extensive validation of a thermodynamically consistent, nonlinear viscoelastic model for glassy polymers, *Polym.* 45 (13) (2004) 4599–4621.
- [28] J.D. Ferry, R.A. Stratton, The free volume interpretation of the dependence of viscosities and viscoelastic relaxation times on concentration, pressure, and tensile strain, *Kolloid-Z.* 171 (2) (1960) 107–111.
- [29] S. Goyanes, W. Salguero, A. Somoza, J.A. Ramos, I. Mondragon, Direct relationships between volume variations at macro and nanoscale in epoxy systems. PALS/PVT measurements, *Polym.* 45 (19) (2004) 6691–6697.
- [30] D. Kilburn, D. Bamford, G. Dlubek, J. Pionteck, M.A. Alam, The size and number of local free volumes in polypropylenes: a positron lifetime and PVT study, *J. Polym. Sci. B: Polym. Phys.* 41 (23) (2003) 3089–3093.
- [31] R.W. Garbella, J. Wachter, J.H. Wendorf, Influence of structural defects on viscoelastic properties of poly(propylene), *Prog. Coll. Polym. Sci.* 71 (1985) 164–172.
- [32] J. Kolařík, A. Pegoretti, L. Fambri, A. Penati, Polypropylene/elastomer/poly(styrene-co-acrylonitrile) blends: manifestation of the critical volume fraction of SAN in dynamic mechanical, tensile and impact properties, *J. Polym. Res.* 7 (1) (2000) 7–14.